International Journal of Nanomedicine

Dovepress
open access to scientific and medical research

Open Access Full Text Article

ORIGINAL RESEARCH

Self-Nanoemulsifying Drug Delivery System-Containing the Poorly Absorbed Drug – Valsartan in Post-Bariatric Surgery

Tzu-Hao Huang[1], Chih-Jung Chen[2–4], Hsin-Chia Angela Lin[1], Chun-Han Chen[1,*], Jia-You Fang[5–7,*]

[1]Division of General Surgery, Department of Surgery, Chang Gung Memorial Hospital, Chiayi, Taiwan; [2]Department of Pathology and Laboratory Medicine, Taichung Veterans General Hospital, Taichung, Taiwan; [3]School of Medicine, Chung Shan Medical University, Taichung, Taiwan; [4]Department of Post-Baccalaureate Medicine, College of Medicine, National Chung Hsing University, Taichung, Taiwan; [5]Graduate Institute of Natural Products, Chang Gung University, Kweishan, Taoyuan, Taiwan; [6]Research Center for Food and Cosmetic Safety, Research Center for Chinese Herbal Medicine, and Graduate Institute of Health Industry Technology, Chang Gung University of Science and Technology, Kweishan, Taoyuan, Taiwan; [7]Department of Anesthesiology, Chang Gung Memorial Hospital, Kweishan, Taoyuan, Taiwan

*These authors contributed equally to this work

Correspondence: Chun-Han Chen, Division of General Surgery, Department of Surgery, Chang Gung Memorial Hospital, Chiayi, 6, W. Sec., Jiapu Road, Puzih City, Chiayi County, 61363, Taiwan, Tel +886-5-3621000 ext. 3821, Fax +886-5-3623002, Email chen5746@cgmh.org.tw; Jia-You Fang, Graduate Institute of Natural Products, Chang Gung University, 259 Wen-Hwa 1st Road, Kweishan, Taoyuan, 333, Taiwan, Tel +886-3-2118800, Fax +886-3-2118236, Email fajy@mail.cgu.edu.tw

Purpose: Morbid obesity and its related metabolic syndrome are an important health issue. Recently, sleeve gastrectomy (SG) and Roux-en-Y gastric bypass (RYGB) have accounted for the most popular bariatric surgeries. Valsartan (VST) is a common hypertension drug, and nano-carriers can increase its solubility and bioavailability. This study aims to explore the nano-VST formula in bariatric surgery subjects.

Methods: High-fat fed animals were used as obese models. Operations were performed according to a standardized protocol. The drug was administrated by gavage, and blood samples were taken by serial tail vein sampling. Caco-2 cells were used for examining cell viability and drug uptake. A self-nano-emusifying drug delivery system (SNEDDS) formula was composed of sefsol-218, RH-40 and propylene glycol by a specified ratio, while high-performance liquid chromatography (HPLC) was used for determining drug concentrations.

Results: Post-operatively, subjects that underwent RYGB lost more body weight compared to the SG group. The SNEDDS did not exhibit cytotoxicity after adequate dilution, and the cytotoxicity was not related to VST dose. A better cellular uptake of SNEDDS was observed in vitro. The SNEDDS formula achieved a diameter of 84 nm in distilled water and 140 nm in simulated gastric fluid. In obese animals, the maximum serum concentration (C_{max}) of VST was increased 1.68-folds by SNEDDS. In RYGB with SUS, the C_{max} was reduced to less than 50% of the obese group. SNEDDS increased the C_{max} to 3.5 folds higher than SUS and resulted in 3.28-folds higher $AUC_{0\text{-}24}$ in the RYGB group. Fluorescence imaging also confirmed a stronger signal of SNEDDS in the gastrointestinal mucosa. SNEDDS accumulated a higher drug concentration than suspension alone in the liver of the obese group.

Conclusion: SNEDDS could reverse the VST malabsorption in RYGB. Further studies are mandatory to clarify post-SG change of drug absorption.

Keywords: gastric bypass, sleeve gastrectomy, valsartan, nano-drug delivery system

Introduction

Morbid obesity is increasing in prevalence globally and is commonly associated with metabolic syndrome. Bariatric surgeries provide sustained effects on weight loss and ameliorate obesity-attributable comorbidities in the majority of morbidly obese patients.[1] Life span extension and life quality improvement after surgery have also been well established in the literature.[2,3] Two major methods are widely accepted as standard treatments of morbid obesity; sleeve gastrectomy (SG) accounts for the most popular bariatric procedure (61% of almost 252,000 surgeries) followed by roux-en-Y gastric

Received: 20 November 2022
Accepted: 14 April 2023
Published: 17 May 2023

bypass (RYGB) (17%.)[4] Traditionally, the weight reduction effect of bariatric surgeries is due to two mechanisms: restriction and malabsorption. However, recent discussions increasingly focus on the effects of gut-brain axis and intestinal microbiota.[5,6] In RYGB, a small gastric pouch (50 mL or less) is created for restriction and a biliopancreatic limb, which diverts bile and pancreatic fluid to the distal bowel is made for fat malabsorption. On the other hand, SG is a restrictive procedure, but some of its gut hormone profile resemble that of RYGB. As a result, bariatric surgeries will inevitably influence several important factors of drug absorption such as: gastric acidity change, poor gastric mixing, poor lipid emulsification, poor lipid absorption and decreasing the effective intestinal surface area. Current literature have shown a great variation of drug absorption after bariatric surgery, and the unpredictability was mainly attributed to factors relating to the patient, drugs and procedures.[7]

Nanomedicine is regarded as "the use of nanoscale material properties and physical characteristics for the diagnosis and treatment of diseases at the molecular level."[8] Nano-drug delivery systems are engineered technologies that use nanoparticles for the targeted delivery, increase therapeutic efficacy and reduce side effects.[9] Nanoparticles can be defined as a material with sizes ranging from 10 to 100 nm. Some of the various nanoparticles such as carbonaceous materials, polymeric micelles, lipid-based nanoparticles, magnetic iron-oxide nanoparticles, nanogels and dendrimers have drawn much attention on their diverse applications.[10,11] Nanoemulsions are a relatively inexpensive strategy, improving bioavailability through its greater surface area and increasing lipophilic drug solubility.[12,13] Self-nanoemulsifying drug delivery system (SNEDDS) is one of the most commonly used lipid-based technology,[14] and SNEDDS has successfully reduced liver steatosis in animal model.[15] However, the application of SNEDDS on SG is still not well known.

Valsartan (VST) is a poorly water-soluble drug commonly used for the treatment of hypertension and hypercholesterolemia which are common in overweight patients. VST is a tetrazole derivative, which is poorly soluble in low pH and soluble in neutral pH with low permeability.[16,17] The solubility/dissolution behavior of VST is one of the key factors to its oral bioavailability. SNEDDS had been used to improve bioavailability of VST in previous studies.[18,19] This study tested the pharmacokinetics and safety of SNEDDS-VST on two bariatric surgery models.

Materials and Methods

Animals

All animal procedures were performed in accordance with protocols approved prospectively by the institute of animal care and use committee of Chang Gung Memorial Hospital, Chiayi, and we followed the guideline for the care and use of laboratory animals, 8th edition, National Academic Press, USA, for the welfare of laboratory animals. Male Sprague-Dawley rats were acquired from Lasco (Taipei, Taiwan) at the age of 6 weeks and acclimatized for at least a week under a strict 12:12-h light–dark cycle with ad libitum access to diet and drinking water. The rats were fed a high-fat diet containing 60% of calories as fat (D12492, Research Diets, NJ, USA) for 6 weeks.

Bariatric Surgery

Animals were fasting for 6–8 hours before operation. Under anesthesia with 1–2% isoflurane (Abbott, IL, USA) in oxygen at the suitable dose and condition, an upper midline laparotomy was performed. The animals underwent either a RYGB or SG. For RYGB, the procedures were performed as previously described[20] and demonstrated in Figure 1a and b. For SG, a 7 Fr. catheter was inserted from mouth to stomach as guidance of standard gastric sleeve. The forestomach was divided along the presumed line between the angle of His and the edge of the glandular stomach at the greater curvature side while preserving the gastroesophageal junction and the pylorus. The gastrostomy was closed using 6–0 Prolene in a continuous fashion (Figure 1c and d). Post-operatively, the animals recovered in a warm cage before returning to the post-operative room. All animals were provided 0.1 mg/kg nalbuphine (Genovate, HsinChu, Taiwan) subcutaneously twice a day for 48 hours as pain relief. The animals were provided Pedialyte (Abbott, IL, USA) for 2 days and then shifted to gel diet (DietGel®76A, ClearH2O, ME, USA) on post-operative day 3 for 4 days. We provided ~2 g of fully crushed HFD in a glass Petri dish on the bottom of the cage in the subsequent 2 days, then on day 7, we

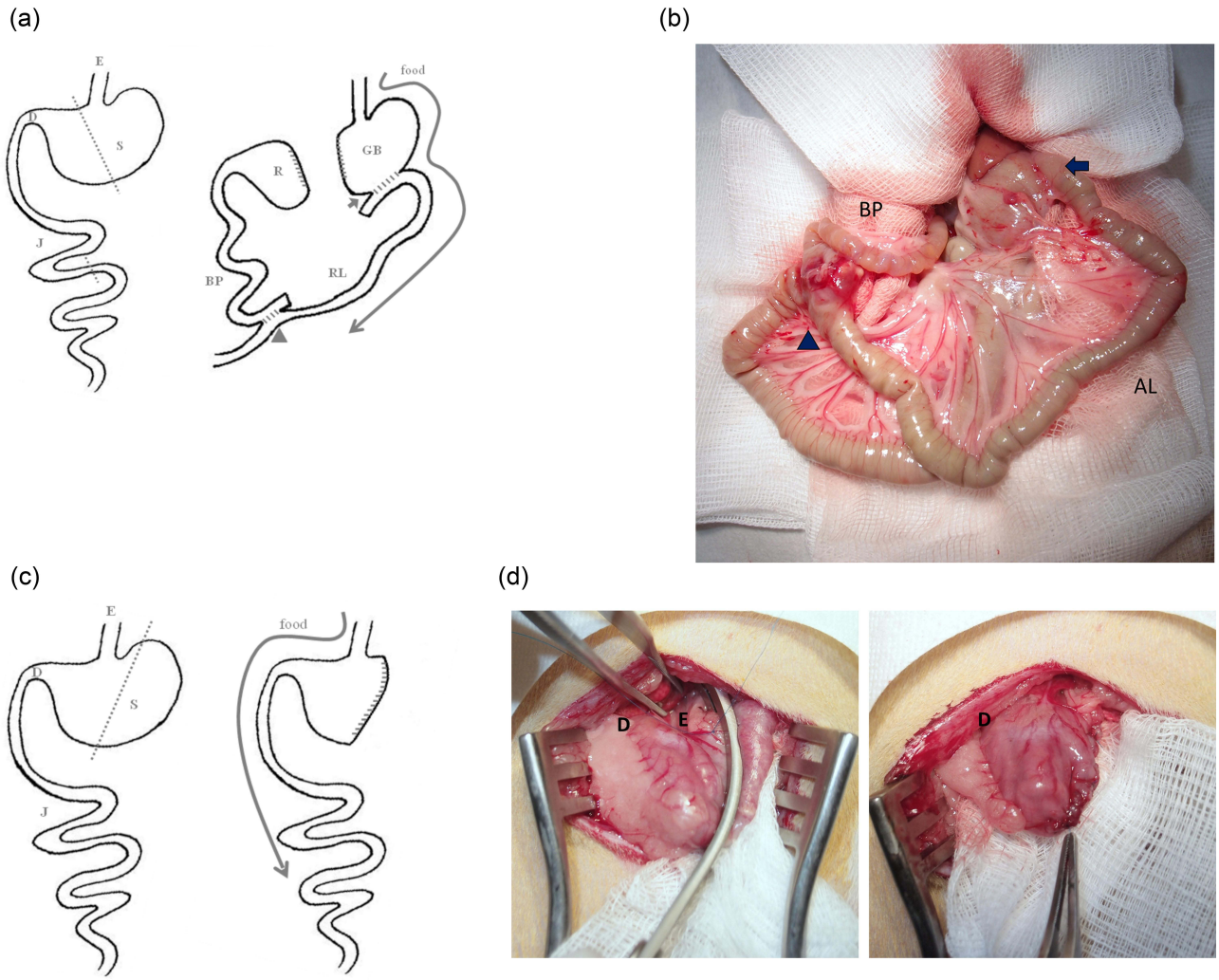

Figure 1 Animal surgery: (**a**) Roux-en-y gastric bypass (RYGB), (**b**) surgery photo of RYGB, (**c**) sleeve gastrectomy (SG), and (**d**) surgery photo of SG.
Notes: Arrow: gastrojejunostomy; triangle: jejunojejunostomy; dot line: resection line; "food and arrow line" indicates food transportation in gastrointestinal tract.
Abbreviations: E, esophagus; S, stomach; D, duodenum; J, jejunum; R, remaining stomach; GP, gastric pouch; BP limb, biliopancreatic limb; AL, alimentary limb.

started transitioning to a solid diet, during which a liquid diet must be provided as well. Pharmacokinetic experiments were performed on the 10th post-operative day.

Drug Suspensions and SNEDDS Preparation

The drugs were suspended in a 1% carboxymethylcellulose sodium (USP) medium. The optimized SNEDDS formulation for VST was modified from a previous study, which for this study, consisted of sefsol-218 as the oil, Cremophor RH40 as the surfactant, and propylene glycol as a cosurfactant, in a proportion of 40% (w/w) oil, 40% surfactant and 20% cosurfactant. The oil and surfactant were heated to 37°C and mixed well before adding to the VST-propylene glycol solution at room temperature for the resulting drug containing a maximum of 10% (w/w) VST.

Droplet Size Analysis

The droplet size of the microemulsions was measured by the means of PCS, using a Zetasizer 3000 (Malvern Instruments, UK). The samples were measured at 37 °C after the addition of 250 mL 37 °C water to 1 g of mixture. No further treatment of the samples was necessary.

Morphology of Lipid Nanocarriers

The size and morphology of SNEDDS and NLC after dilution were visualized by transmission electron microscopy (TEM). A drop of the diluted nanoemulsion was deposited onto a grid to produce a thin-film sample and then stained with 0.5% phosphotungstic acid. The specimen were monitored by a TEM (H7500, Hitachi).

Pharmacokinetics (PK)

The animals were fasted overnight for 6–8 hours. After gavage administration of a standard dose of VST (4 mg/kg), about 0.3 mL of blood samples were collected through the tail vein into EDTA coated tubes (Becton Dickinson, Taiwan) at 0, 0.5, 1, 1.5, 2, 4, 8, 12, and 24 h. Blood samples were centrifuged at 3000 rpm at 4 °C for 10 min using a refrigerated centrifuging machine (Model 5500, Kubota, Japan) and the plasma was aspirated and stored at −20 °C. Serum drug levels were determined by high-performance liquid chromatography (HPLC). VST separation was achieved by C-18 column (Macherey-Nagel, Duren, Germany) (4.6 × 250mm; 5μm) using acetonitrile and disodium hydrogen phosphate buffer (pH 3.2) as mobile phase in a ratio of 60:40. The mobile phase was eluted into a column with 1.5 mL/min flow rate with a fixed temperature of 30°C. Estimation of VST was monitored by fluorescent detector at 255 nm (Excitation) and 370 nm (Emission).

Fluorescent Microscopy

The fluorescent labeled drugs were prepared with Nile red (Sigma-Aldrich, Shanghai, China) diluted in 1:1000 w/w ratio with specified solutions the night before administration. After gavage of the fluorescently labeled drugs, the animals were sacrificed and organs were harvested at specified timings. After gentle irrigation with 0.9% sodium chloride, the specimen were put into an embedding medium (O.C.T. compound; Sakura, Tokyo, Japan) and rapidly frozen. Frozen sections were cut serially at a thickness of 5–6 μm. DAPI (Invitrogen, Taipei, Taiwan) was then used for nuclear staining. The slides were imaged by confocal microscopy (TSC SP5, Leica, Wetzlar, Germany), and the images were captured and processed with the Leica AF software (version 2.6.3 build 8173).

Cell Culture

CaCo-2 cells were obtained from the Bioresource Collection and Research Center (Hsinchu, Taiwan) and used between passages 20 and 35. Cells were cultured in Dulbecco's modified Eagle medium (D-MEM, high glucose) and supplemented with 10% (v/v) fetal bovine serum, 1% (w/v) human transferrin, 1% (v/v) sodium pyruvate, and 1% antibiotic solution (1×104UI/mL penicillin, 10 mg/mL streptomycin, 25 μg/mL amphotericin B) in a humidified incubator with 5% CO2/95% air at 37 °C. Cell proliferation was detected by water-soluble tetrazolium salt WST-8. Cells (5000/well) were seeded into 96-well plates and cultured for 1 week. Each preconcentrate was diluted serially with culture medium to produce test concentrations, which were then added to individual wells at the volume of 100 μL per well, followed by incubation for 0.5 h. A total of 10 μL CCK-8 (TargetMol) was then added to each well and the plate was incubated for 2h at 37°C until the color turned orange. The absorbance was then measured with a microplate ELISA reader at 450 nm. Qualitative uptake of SNEDDS in CaCo-2 cells were measured by fluorescence microscope. CaCo-2 cells were seeded into 6-well plates for 24 h. On reaching 80% confluence, the culture medium was replaced with PBS. After 30 min of incubation at 37 °C, cell monolayers were washed three times with PBS. The cells were incubated with 0.5 ng/mL Nile red solution and Nile red-SNEDDS for 2 hours. Then, the cells were rinsed 3 times with PBS, after which the cells were observed by fluorescence microscopy.

Statistics

The pharmacokinetics data were analyzed by Phoenix WinNonlin V8.1 software (Certara, St. Louis, MO, USA). All data were expressed as the mean ± standard deviation (SD). Statistical analyses were performed using independent Student's t-test and Chi-square test in quantitative and categorical variables, respectively. Differences were considered significant at $p < 0.05$.

Results

The body weight change among the post-operative obese animals was significantly different since post-OP Day 1 (Figure 2). The body weight reduction by RYGB was sustainably more than SG since POD2 ($p = 0.010$) till the end of experiment (POD14) ($p = 0.002$). The maximum weight reduction rates were 14% (POD 8) and 22% (POD9) in SG and RYGB when compared to obese rats, respectively.

The SNEDDS formulation results in clear and transparent appearance, neither phase separation nor precipitation on emulsion, could be found based on visual assessment. Physicochemical profiles of SNEDDS are demonstrated in Table 1 after diluting 100-fold in water and simulated gastric juice. The mean size of oil droplets reached 84 nm and carried a negative surface charge (−5.44 mV) in water. The droplet size was increased (140 nm) when SNEDDS was dissolved in simulated gastric juice and surface charge became low positive (0.18 mV). The oil droplets of SNEDDS could be visualized by transmission electron microscopy as seen in Figure 3. The oil droplets were spherical in shape and slightly varied in size (Figure 3a), and while the droplets were mostly separated, aggregation was also observed at a higher magnification (Figure 3b).

The viability rates of CaCo-2 cell monolayer cultured 2 hours in aqueous suspension (SUS) and SNEDDS were not statistically significant after diluting more than 2000-fold (Figure 4a). After adequate dilution, the cell viability showed no difference in VST concentrations ranging from 0.5 to 10 μg/mL (Figure 4b). The confocal fluorescence microscopy revealed better intracellular red stain in Nile red labeled SNEDDS than SUS 2 hours after drug administration (Figure 5).

The pharmacokinetic parameters of SNEDDS and SUS in different surgical groups ($n = 5$~9) are shown in Table 2. The C_{max} of SUS in obese, SG and RYGB rats was 2.64, 1.94 and 1.26 μg/mL, respectively, where RYGB results in a 47.8% C_{max} reduction compared to control ($p < 0.001$). The $AUC_{0\text{-}24}$ in different groups are summarized in Figure 6. The $AUC_{0\text{-}24}$ of SUS was 38.95, 49.43 and 35.45 μg*hours/mL in obese, SG and RYGB, respectively, and yielded no statistical significance. In the obese group, the C_{max} and $AUC_{0\text{-}24}$ of SNEDDS were 4.43 μg/mL and 50.99 μg*hours/mL, respectively. Although the C_{max} of SNEDDS increased 1.7-fold higher than SUS ($p = 0.008$), the $AUC_{0\text{-}24}$ was not statistically different between SUS and SNEDDS in this group. In RYGB, the C_{max} of SNEDDS was 3.5-fold higher than SUS ($p < 0.001$); the $AUC_{0\text{-}24}$ of SNEDDS was also significantly higher than SUS (116.11 vs 35.45 μg*hours/mL, $p = 0.019$), indicating that SNEDDS exhibited a 3.3-fold greater bioavailability after RYGB. Furthermore, the $AUC_{0\text{-}24}$ of SNEDDS in RYGB was also significantly higher than SNEDDS in the obese group ($p = 0.049$). Figure 7 shows the plasma concentration–time profiles in different groups. The T_{max} of SUS occurred in 2 hours in obese

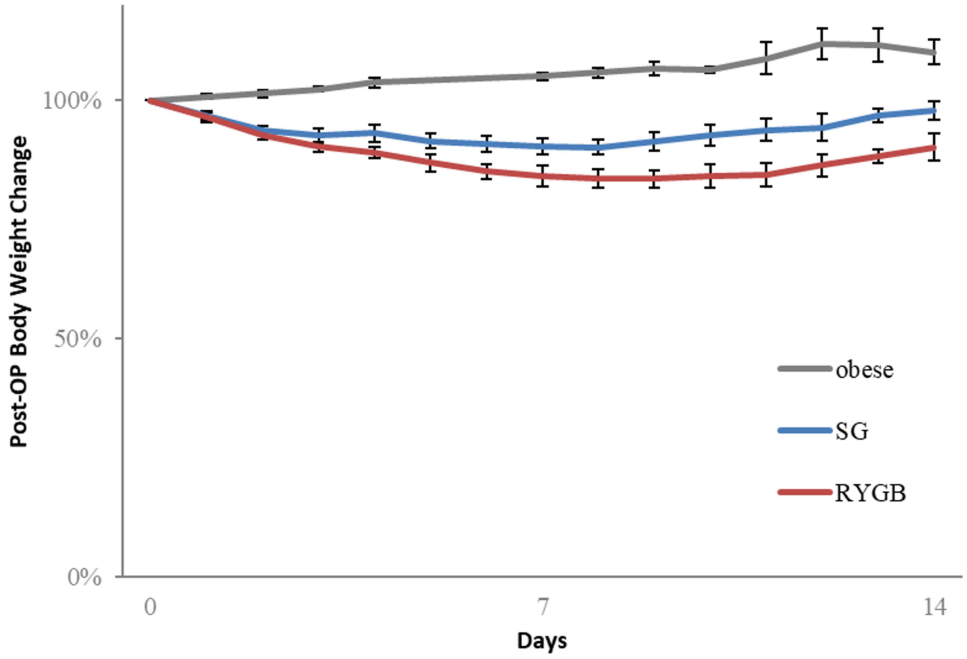

Figure 2 Body weight change of SG and RYGB operation. Each value represents the mean and S.D. (n = 6 to 10).

Table 1 Characterization of Valsartan SNEDDS

SNEDDS	Size (nm)	Polydispersity Index	Zeta Potential (mV)
In water	83.67 (± 30.24)	0.29 (± 0.06)	−9.36 (± 1.05)
In simulated gastric fluid	141.83 (± 26.12)	0.17 (± 0.05)	−0.21 (± 1.01)

Note: Each value represents the mean ± standard deviation.

rats but delayed to 3 hours in RYGB (Figure 7a). However, T_{max} of SUS reduced to less than 1 hour in SG with a wider range of variation (Table 2). After administering with SNEDDS, the T_{max} occurred within 1 hour in all three groups but variation persisted in SG and RYGB groups (Figure 7b, Table 2). The serum concentration of SNEDDS showed faster elimination after 12 hours in obese rats. Although the SNEDDS concentration–time curve seems to be separated from SUS in SG, the statistical examinations yielded no difference in C_{max} and $AUC_{0\text{-}24}$ due to intragroup variation (Table 2). On the contrary, SNEDDS increased serum concentration at each time point throughout the tested period in RYGB. Drug distribution at 24 hours after administration in obese rats reveals that the liver accumulated 12.38 (± 2.47) and 4.72 (± 2.54) μg/g VST in SNEDDS and SUS, respectively ($p = 0.039$). There were no differences between SG and RYGB groups on VST tissue distribution at 24 hours.

The pH analysis of gastric fluid before drug administration yielded a higher ratio of pH >5 in RYGB (37.5%) than obese (12.5%) and SG (9.1%) ($p = 0.102$ and 0.034, respectively).

The GI uptake of fluorescence labeled drugs 2 hours after drug administration is demonstrated in Figure 8. Nile-red labeled SNEDDS showed a better transmural infiltration than suspension, either in stomach or intestine of obese rats.

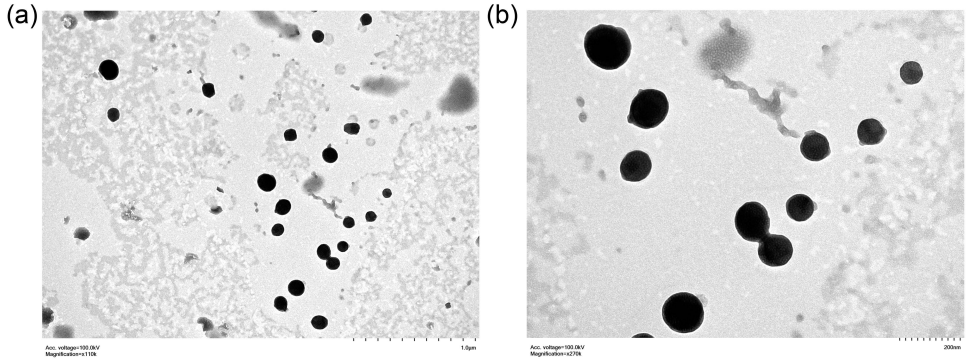

Figure 3 Transmission electron microscopy of SNEDDS. (**a**) Magnification: x110k, (**b**) magnification x270k.

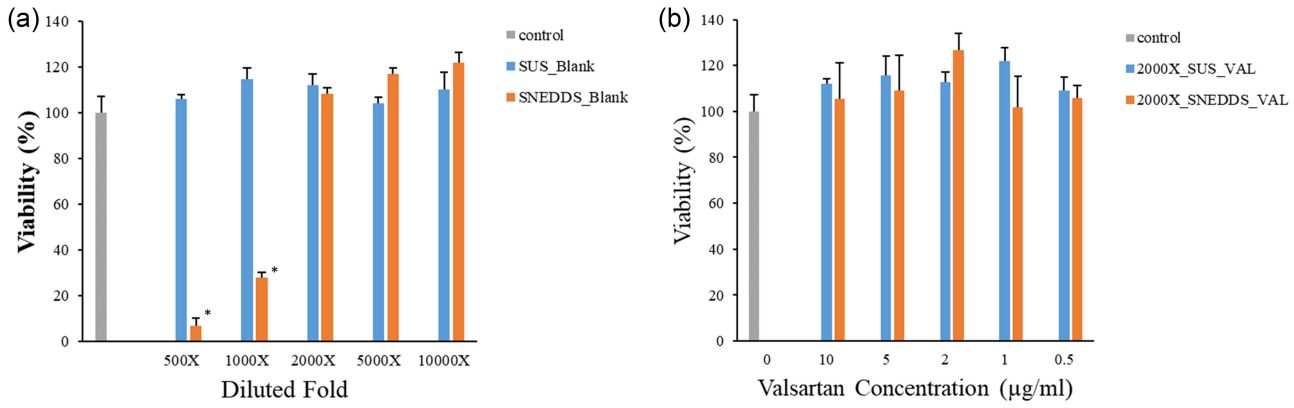

Figure 4 Viability of Caco2 cells. (**a**) Culture 2 hours in different formula, (**b**) culture in formula loaded with Valsartan. *: $p < 0.05$, statistically significant between suspension and SNEDDS at the same dilution.

Abbreviations: SUS_Blank, 1% carboxymethylcellulose sodium suspension medium; SNEDDS_Blank, unloaded SNEDDS; SUS_VAL, valsartan aqueous suspension; SNEDDS_VAL, valsartan loaded SNEDDS.

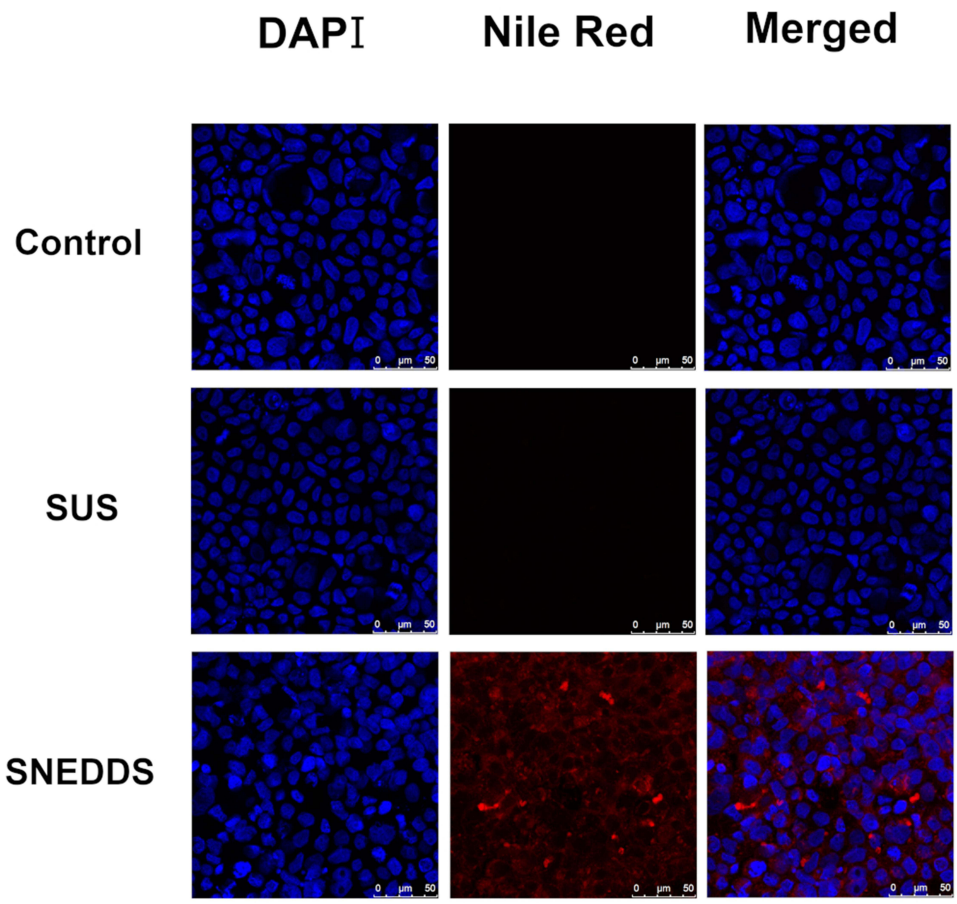

Figure 5 Caco2 monolayer uptake of Nile-red labeled drugs (0.5μg/mL).

A weakly positive stain could be found in SG stomach, but not in RYGB. On the contrary, on the intestinal mucosa of RYGB rats, the fluorescence intensity appeared to be stronger than SG.

The histology and immunohistochemistry stains for PCNA and Cox-2 after animal were sacrificed are demonstrated in Figure 9. No evidence of mucosal damage could be identified on histological exams in either SUS or SNEDDS group. IHC stain of PCNA or Cox-2 also revealed no obvious mucosal inflammatory responses after SNEDDS.

Table 2 Pharmacokinetic Parameters of Valsartan (4 mg/kg) After Oral Administration from Suspension and SNEDDS in (a) Obese, (b) SG and (c) RYGB Rats

(a)		
	Suspension (n = 7)	**SNEDDS (n = 8)**
C_{max} (μg/mL)	2.64 (± 0.22)	4.43 (± 0.33)
T_{max} (hours)	2.28 (± 0.47)	1.71 (± 0.38)
AUC_{0-24} (μg*hours/mL)	38.95 (± 8.24)	50.99 (± 10.00)
Clearance (mL/hour/kg)	102.68 (± 21.73)	78.45 (± 15.41)

(*Continued*)

Table 2 (Continued).

(b)		
	Suspension (n = 9)	**SNEDDS (n = 8)**
C_{max} (μg/mL)	1.94 (± 0.60)	5.61 (± 19.51)
T_{max} (hours)	0.93 (± 7.07)	0.74 (± 32.75)
AUC_{0-24} (μg*hours/mL)	49.43 (± 15.95)	72.08 (± 28.13)
Clearance (mL/hour/kg)	80.92 (± 26.13)	55.49 (± 21.68)
(c)		
	Suspension (n = 5)	**SNEDDS (n = 6)**
C_{max} (μg/mL)	1.26 (± 0.07)	4.43 (± 5.74)
T_{max} (hours)	3.10 (± 0.78)	0.81 (± 28.12)
AUC_{0-24} (μg*hours/mL)	35.45 (± 6.84)	116.11 (± 21.36)
Clearance (mL/hour/kg)	112.83 (±21.81)	34.45 (± 6.34)

Note: Each value represents the mean ± standard error.
Abbreviations: AUC_{0-24}, area under the curve 0–24 hours; C_{max}, maximum serum concentration; $T_{max,}$ time to maximum concentration.

Discussion

Our animal model suggests that RYGB is a more effective surgery in terms of weight reduction than SG, which is very similar to clinical practice.[21] However, the animal model presented with some limitation when representing human surgery. First, the gastric tube cannot be created as small as human surgeries due to a harder rodent diet and shorter food transition time than human. Second, the rodent stomach was anatomically divided into glandular and non-glandular stomach with a clear watershed, which does not exist in humans.

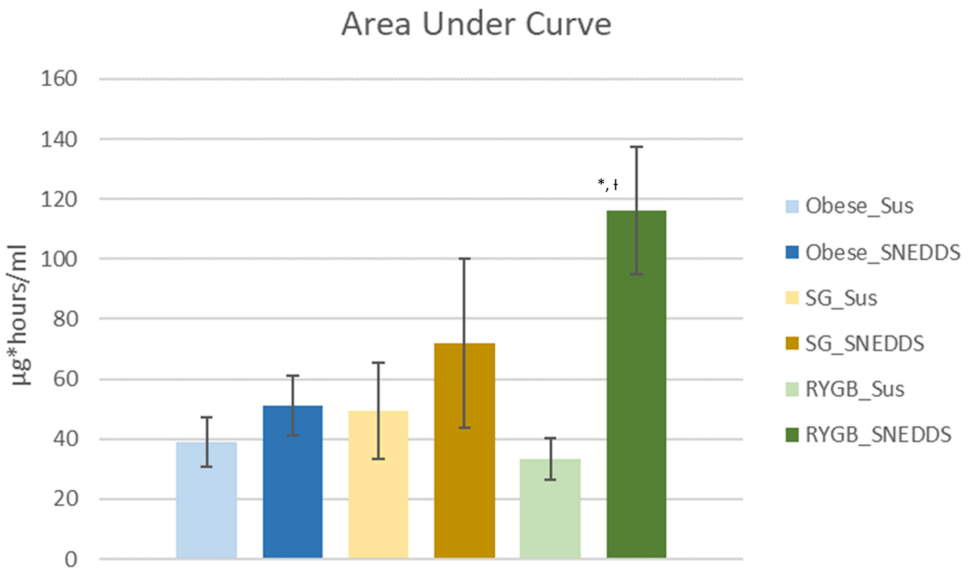

Figure 6 Area under curve (AUC_{0-24}) of the plasma concentration–time curves. Each value represents the mean and standard error (n= 5~9).
Notes: *Statistically significant ($p < 0.05$) when compared with SNEDDS in obese rats. [ł]Statistically significant ($p < 0.05$) when compared with suspension in RYGB rats.
Abbreviations: Obese_Sus, valsartan suspension in obese rats; Obese_SNEDDS, valsartan SNEDDS in obese rats; SG_Sus, valsartan suspension in SG; SG_SNEDDS, valsartan SNEDDS in SG; RYGB_Sus, valsartan suspension in RYGB; RYGB_SNEDDS, valsartan SNEDDS in RYGB.

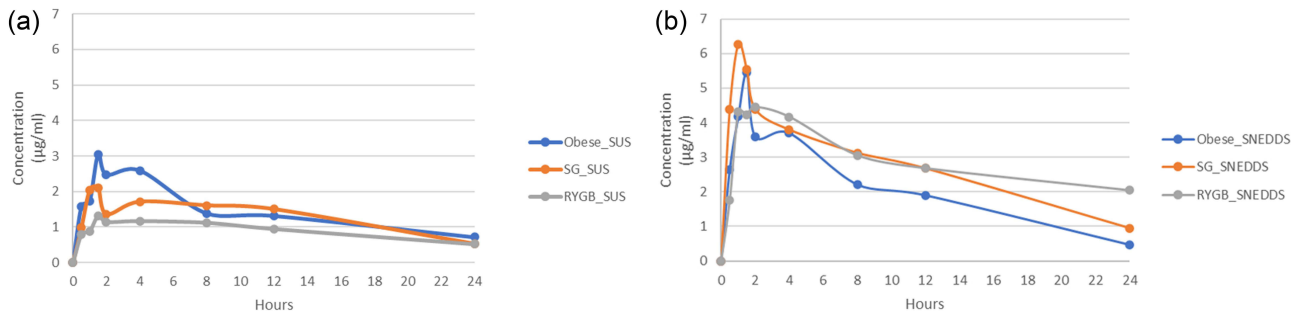

Figure 7 Plasma concentration of valsartan versus time curves: (**a**) suspension (SUS) in different groups, (**b**) SNEDDS in different groups. Each value represents the mean and standard error (n = 5~9).

Abbreviations: Obese_SUS, valsartan suspension in obese rats; Obese_SNEDDS, valsartan SNEDDS in obese rats; SG_SUS, valsartan suspension in SG; SG_SNEDDS, valsartan SNEDDS in SG; RYGB_SUS, valsartan suspension in RYGB; RYGB_SNEDDS, valsartan SNEDDS in RYGB.

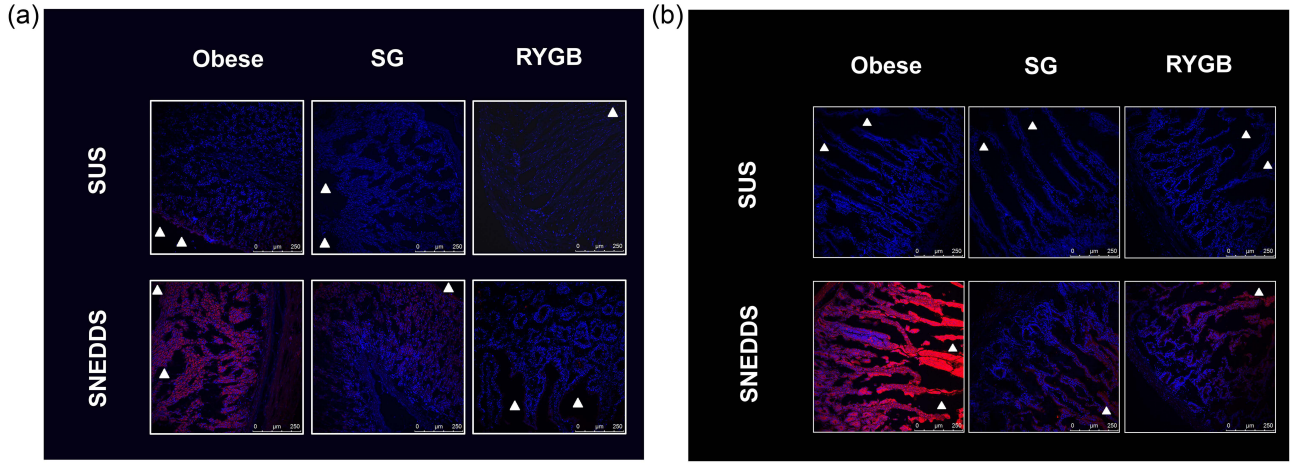

Figure 8 The fluorescence microscopic image 2 hours after oral administration of Nile red labeled suspension (SUS) and SNEDDS in (**a**) stomach and (**b**) small intestine of obese, SG and RYGB. Triangles indicate the lumens.

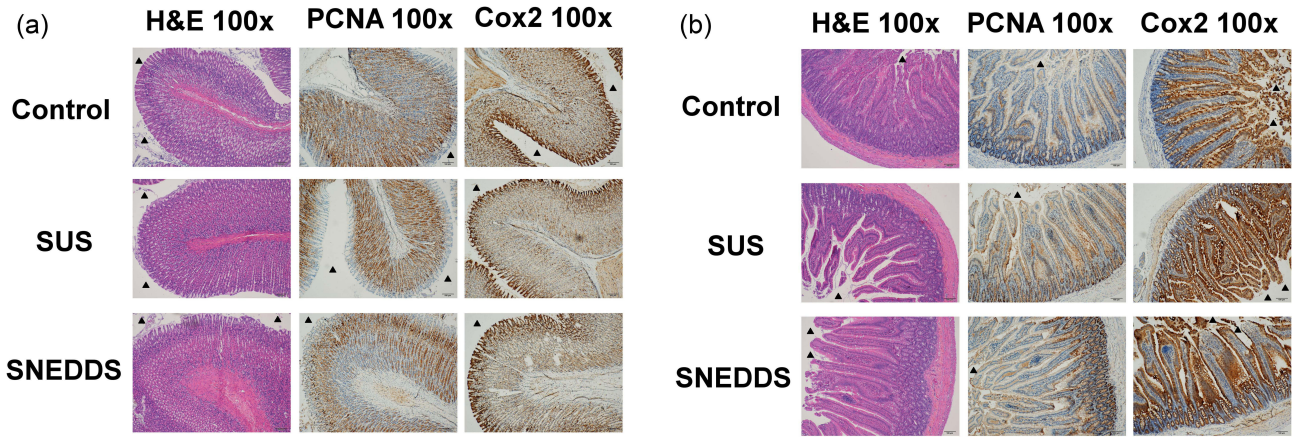

Figure 9 Immunohistochemistry stain of gastrointestinal tract 24 hours after drug oral gavage: (**a**) stomach, (**b**) small intestine of obese, SG and RYGB. Triangles indicate the lumens.

One particular issue after bariatric surgery is the change of proximal gastrointestinal tract acidity. On increasing pH from 4 to 6, the VST solubility increases but lipophilicity (permeability) decreases. RYGB mainly prevents acidic environment from contact with drugs, while SG excised only the storage zone of stomach. RYGB contained not only a relatively alkaline gastric pouch for drug absorption but also provided a stable pH in the alimentary limb when the biliopancreatic limb was designed to be far from the gastrojejunostomy on purpose. The SUS-VST dissolved after oral administration in the RYGB group but had poor penetration into the mucosa. On the contrary, negatively charged nano-vesicle aggregation could be prevented in the gastric pouch of RYGB, while nano-lipid droplets increased contact surface area and mucosa absorption. In this study, high pH >5 could be detected in one-third of the RYGB gastric fluid samples. We hypothesize that the relatively neutral-basic proximal alimentary tract of RYGB might be beneficial to VST nanocarrier's stability and contributed to the increased bioavailability.

Furthermore, the change in gastric emptying time may have a major impact on drug absorption. Animal studies have revealed a faster gastric emptying time in both SG and RYGB than control.[22] Most human studies also confirmed a faster gastric emptying after SG.[23] We believe that the T_{max} variation of both SUS and SNEDDS in SG could be explained by post-operative change of gastric motility. SUS-VST is not easily dissolved in acidic gastric fluid and is rapidly passed into the duodenum, which may result in variable drug absorption in SG. We expected a lower C_{max} of SUS in SG than the obese group. Contact of non-ionic surfactant (Rh40) containing oil droplets to bile salts in the duodenum would change the solubility of SNEDDS-VST significantly. The dependence of drug solubility on surfactant–bile interactions had been demonstrated in a previous study.[24] Furthermore, the acidity in the stomach might be unfavorable for SNEDDS, as simulated gastric juice enlarged droplet size and decreased surface-negative potential. Altogether, gastrointestinal pH, fast gastric emptying and nanoparticle–bile interaction contributed to the unpredictable outcomes of SNEDDS in SG.

Food stasis could be another rationale of our pharmacokinetics' variation. We used a high-fat diet to develop obesity and metabolic diseases in our animals, as it is a reliable method; however, high fat contenting food stasis inside stomach/proximal intestine might interfere with the behavior of nano-oil droplets. Gastric stasis and dysphagia have been reported to be post-operative problems occurring in both SG and RYGB patients.[25,26] In addition, as rodents are nocturnal animals, diet remnant inside the proximal gastrointestinal tract despite "nil per os" was not an uncommon finding in animal experiments during daytime.

Although SNEDDS is easy to prepare, the high amount of surfactant required remained a major disadvantage. Rh40 increases mucosal drug absorption through the inhibition of P-glycoprotein efflux and cytochrome P450 activity in the gut, and the cytotoxicity effect of Rh40 had been found to be positively related to cell permeation.[27,28] Some surfactant substitutes had been shown to reduce Rh40 toxicity in vitro.[29] Various nanoformulae had been evaluated on increasing the bioavailability of VST; SNEDDS had shown an expectable result throughout different nano-drug delivery systems.[30] The acceptable size range of SNEDDS droplets is between 20 and 200 nm,[31] while our formula was able to form nanodroplets in simulated gastric juice (pH 1.2) with a mild size increase. The aggregation of droplets observed on TEM could be attributed to the low negative zeta potential.[9] One major drawback of SNEDDS is its low drug loading capacity, but a new class of supersaturable formulation had been designed to overcome it.[32] Notably, the highly variable scaffolds of carbon nanofiber drug delivery systems could be another plausible solution to increase poorly water-soluble drug absorption in post-bariatrics.[33] However, the applicability of different drug delivery systems on bariatric surgery is not yet elucidated and warrants further research.

In this study, fluorescence labeled SNEDDS stained intestinal mucosa better than stomach in all three groups at a specific timing after drug administration. The increased drug absorption of SNEDDS could be explained due to better intestinal mucosa permeation of nanoparticles. However, in the histological examination, we found no evidence of mucosal damage in both H&E and IHC staining after a single dosage. A longer period of observation with regular doses of SNEDDS should be mandate for cytotoxic effects of undiluted nano-carriers occurring in vitro.

A low serum VST concentration was found 12 hours after SNEDDS administration in obese animal. Significant fatty liver disease could be observed after a high-fat diet for 6 weeks in rats. The lipid accumulation in liver of obese animals could be rapidly reversed by RYGB.[15] Similar improvement of fatty liver disease after SG was observed in human studies on both image and histological evaluation.[34] The finding that both SG and RYGB significantly improved fatty liver disease of diabetic patients was published in a recent randomized trial.[35] In obese animals, the liver accumulation of

VST by SNEDDS could be attributed to the interaction of lipophilic SNEDDS and fatty liver. Mechanism known as passive liver targeting of lipid nanoparticles including particle size about 40–150 nm and enterohepatic circulation had been proposed in the literature.[36,37] While VST is mainly excreted in bile,[17] liver accumulation could result in faster elimination, which could lead to a comparable $AUC_{0\text{-}24}$ between SNEDDS and SUS in obese animals. However, we have omitted half-life calculation for the limitation of our available drug level beyond 24 hours to avoid controversies.

As demonstrated in our previous study,[20] SNEDDS could ameliorate the RYGB effect on poor absorption of a poor water-soluble drug. Our present study reproduced this phenomenon. However, to our knowledge, this is the first time SG was considered as a target of nanomedicine. Our SNEDDS formula did not successfully increase VST absorption in SG, but we did recognize some important post-operative characteristics that would interfere with drug absorption. If one of the marketed SNEDDS formulae (such as Ritonavir, Tipranavir, Isotretinoin, Sirolimus, Cyclosporin A, Fenofibrate and Bexarotene[38,39]) are going to be used in SG patients, a few concerns should be taken into account, such as: the reduced gastric volume may interfere with the SNEDDS emulsifying progress and the faster gastric motility would mean contact of drugs with bile (and lipolytic enzymes) earlier than normal.

Conclusion

In conclusion, SNEDDS could increase VST absorption after RYGB. Further studies are required for better understanding post-SG change of drug absorption.

Acknowledgments

The authors are grateful for the financial support of Chang Gung Memorial Hospital (grants CMRPG6H0181, CMRPG6J0022 and CMRPG6H0581). We also thank for the assistance of Laboratory Animal Center, Precious Instrumentation Core Laboratory, and Common Laboratory, Chang Gung Memorial Hospital, Chiayi.

Disclosure

The authors report no conflicts of interest in this work.

References

1. Chang SH, Stoll CR, Song J, Varela JE, Eagon CJ, Colditz GA. The effectiveness and risks of bariatric surgery: an updated systematic review and meta-analysis, 2003-2012. *JAMA Surg*. 2014;149(3):275–287. doi:10.1001/jamasurg.2013.3654
2. Adams TD, Gress RE, Smith SC, et al. Long-term mortality after gastric bypass surgery. *N Engl J Med*. 2007;357(8):753–761. doi:10.1056/NEJMoa066603
3. Lindekilde N, Gladstone BP, Lubeck M, et al. The impact of bariatric surgery on quality of life: a systematic review and meta-analysis. *Obes Rev*. 2015;16(8):639–651. doi:10.1111/obr.12294
4. Arterburn DE, Telem DA, Kushner RF, Courcoulas AP. Benefits and risks of Bariatric Surgery in Adults: a Review. *JAMA*. 2020;324(9):879–887. doi:10.1001/jama.2020.12567
5. Cornejo-Pareja I, Molina-Vega M, Gomez-Perez AM, Damas-Fuentes M, Tinahones FJ. Factors related to weight loss maintenance in the medium-long term after bariatric surgery: a review. *J Clin Med*. 2021;10:8. doi:10.3390/jcm10081739
6. Georgiou K, Belev NA, Koutouratsas T, Katifelis H, Gazouli M. Gut microbiome: linking together obesity, bariatric surgery and associated clinical outcomes under a single focus. *World J Gastrointest Pathophysiol*. 2022;13(3):59–72. doi:10.4291/wjgp.v13.i3.59
7. Alalwan AA, Friedman J, Alfayez O, Hartzema A. Drug absorption in bariatric surgery patients: a narrative review. *Health Sci Rep*. 2022;5(3):e605. doi:10.1002/hsr2.605
8. Kim BY, Rutka JT, Chan WC. Nanomedicine. *N Engl J Med*. 2010;363(25):2434–2443. doi:10.1056/NEJMra0912273
9. Miyazawa T, Itaya M, Burdeos GC, Nakagawa K, Miyazawa T. A critical review of the use of surfactant-coated nanoparticles in nanomedicine and food nanotechnology. *Int J Nanomedicine*. 2021;16:3937–3999. doi:10.2147/IJN.S298606
10. Su S, Recent PMK. Advances in nanocarrier-assisted therapeutics delivery systems. *Pharmaceutics*. 2020;12:9. doi:10.3390/pharmaceutics12090837
11. Mamidi N, Velasco Delgadillo RM, Barrera EV, Ramakrishna S, Annabi N. Carbonaceous nanomaterials incorporated biomaterials: the present and future of the flourishing field. *Composites Part B*. 2022;243:110150. doi:10.1016/j.compositesb.2022.110150
12. Jaiswal M, Dudhe R, Sharma PK. Nanoemulsion: an advanced mode of drug delivery system. *Biotech*. 2015;5(2):123–127. doi:10.1007/s13205-014-0214-0
13. Ashaolu TJ. Nanoemulsions for health, food, and cosmetics: a review. *Environ Chem Lett*. 2021;19(4):3381–3395. doi:10.1007/s10311-021-01216-9
14. Kumar R. Lipid-based nanoparticles for drug-delivery systems. *Nanocarriers Drug Delivery*. 2019;1:249–284.
15. Chen CH, Chen CJ, Elzoghby AO, Yeh TS, Fang JY. Self-assembly and directed assembly of lipid nanocarriers for prevention of liver fibrosis in obese rats: a comparison with the therapy of bariatric surgery. *Nanomedicine*. 2018;13(13):1551–1566. doi:10.2217/nnm-2018-0001
16. Wu CY, Benet LZ. Predicting drug disposition via application of BCS: transport/absorption/ elimination interplay and development of a biopharmaceutics drug disposition classification system. *Pharm Res*. 2005;22(1):11–23. doi:10.1007/s11095-004-9004-4

17. Flesch G, Muller P, Lloyd P. Absolute bioavailability and pharmacokinetics of valsartan, an angiotensin II receptor antagonist, in man. *Eur J Clin Pharmacol*. 1997;52(2):115–120. doi:10.1007/s002280050259
18. Amin MM, El Gazayerly ON, Abd El-Gawad NA, Abd El-Halim SM, El-Awdan SA. Effect of formulation variables on design, in vitro evaluation of valsartan SNEDDS and estimation of its antioxidant effect in Adrenaline-induced acute myocardial infarction in rats. *Pharm Dev Technol*. 2016;21(8):909–920. doi:10.3109/10837450.2015.1078354
19. Nekkanti V, Wang Z, Betageri GV. Pharmacokinetic evaluation of improved oral bioavailability of valsartan: proliposomes versus self-nanoemulsifying drug delivery system. *AAPS PharmSciTech*. 2015;1:4532.
20. Chen CH, Chang CC, Shih TH, Aljuffali IA, Yeh TS, Fang JY. Self-nanoemulsifying drug delivery systems ameliorate the oral delivery of silymarin in rats with Roux-en-Y gastric bypass surgery. *Int J Nanomedicine*. 2015;10:2403–2416. doi:10.2147/IJN.S79522
21. Maciejewski ML, Arterburn DE, Van Scoyoc L, et al. Bariatric surgery and long-term durability of weight loss. *JAMA Surg*. 2016;151 (11):1046–1055. doi:10.1001/jamasurg.2016.2317
22. Chambers AP, Smith EP, Begg DP, et al. Regulation of gastric emptying rate and its role in nutrient-induced GLP-1 secretion in rats after vertical sleeve gastrectomy. *Am J Physiol Endocrinol Metab*. 2014;306(4):E424–32. doi:10.1152/ajpendo.00469.2013
23. Sioka E, Tzovaras G, Perivoliotis K, et al. Impact of laparoscopic sleeve gastrectomy on gastrointestinal motility. *Gastroenterol Res Pract*. 2018;2018:4135813. doi:10.1155/2018/4135813
24. Vinarov Z, Katev V, Burdzhiev N, Tcholakova S, Denkov N. Effect of surfactant-bile interactions on the solubility of hydrophobic drugs in biorelevant dissolution media. *Mol Pharm*. 2018;15(12):5741–5753. doi:10.1021/acs.molpharmaceut.8b00884
25. Nath A, Yewale S, Tran T, Brebbia JS, Shope TR, Koch TR. Dysphagia after vertical sleeve gastrectomy: evaluation of risk factors and assessment of endoscopic intervention. *World j Gastroenterol*. 2016;22(47):10371–10379. doi:10.3748/wjg.v22.i47.10371
26. Swartz DE, Gonzalez V, Felix EL. Anastomotic stenosis after Roux-en-Y gastric bypass: a rational approach to treatment. *Surg Obesity Related Dis*. 2006;2(6):632–636. doi:10.1016/j.soard.2006.08.010
27. Khan S, Khan S, Baboota S, Ali J. Immunosuppressive drug therapy--biopharmaceutical challenges and remedies. *Expert Opin Drug Deliv*. 2015;12(8):1333–1349. doi:10.1517/17425247.2015.1005072
28. Bandivadekar M, Pancholi S, Kaul-Ghanekar R, Choudhari A, Koppikar S. Single non-ionic surfactant based self-nanoemulsifying drug delivery systems: formulation, characterization, cytotoxicity and permeability enhancement study. *Drug Dev Ind Pharm*. 2013;39(5):696–703. doi:10.3109/03639045.2012.687745
29. Gao H, Wang M, Sun D, et al. Evaluation of the cytotoxicity and intestinal absorption of a self-emulsifying drug delivery system containing sodium taurocholate. *Eur J Pharm Sci*. 2017;106:212–219. doi:10.1016/j.ejps.2017.06.005
30. Sharma M, Sharma R, Jain DK. Nanotechnology based approaches for enhancing oral bioavailability of poorly water soluble antihypertensive drugs. *Scientifica*. 2016;2016:8525679. doi:10.1155/2016/8525679
31. Date AA, Desai N, Dixit R, Nagarsenker M. Self-nanoemulsifying drug delivery systems: formulation insights, applications and advances. *Nanomedicine*. 2010;5(10):1595–1616. doi:10.2217/nnm.10.126
32. Yeom DW, Chae BR, Son HY, et al. Enhanced oral bioavailability of valsartan using a polymer-based supersaturable self-microemulsifying drug delivery system. *Int J Nanomedicine*. 2017;12:3533–3545. doi:10.2147/IJN.S136599
33. Mamidi N, Garcia RG, Martinez JDH, et al. Recent advances in designing fibrous biomaterials for the domain of biomedical, clinical, and environmental applications. *ACS Biomater Sci Eng*. 2022;8(9):3690–3716. doi:10.1021/acsbiomaterials.2c00786
34. Batman B, Altun H, Simsek B, Aslan E, Koc SN. The effect of laparoscopic sleeve gastrectomy on nonalcoholic fatty liver disease. *Surg Laparosc Endosc Percutan Tech*. 2019;29(6):548–549. doi:10.1097/SLE.0000000000000713
35. Seeberg KA, Borgeraas H, Hofso D, et al. Gastric bypass versus sleeve gastrectomy in type 2 diabetes: effects on hepatic steatosis and fibrosis: a randomized controlled trial. *Ann Intern Med*. 2022;175(1):74–83. doi:10.7326/M21-1962
36. Kasuya T, Kuroda S. Nanoparticles for human liver-specific drug and gene delivery systems: in vitro and in vivo advances. *Expert Opin Drug Deliv*. 2009;6(1):39–52. doi:10.1517/17425240802622096
37. Zhang Z, Li H, Xu G, Yao P. Liver-targeted delivery of insulin-loaded nanoparticles via enterohepatic circulation of bile acids. *Drug Deliv*. 2018;25 (1):1224–1233. doi:10.1080/10717544.2018.1469685
38. Buya AB, Beloqui A, Memvanga PB, Self-nano-emulsifying drug-delivery systems: from the development to the current applications and challenges in oral drug delivery. *Pharmaceutics*. 2020;12(12):1194. doi:10.3390/pharmaceutics12121194
39. Saikumar D, Prasanna JL. A literature review on self nanoemulsifying drug delivery system (SNEDDS). *Int J Pharm Sci Rev Res*. 2021;70:85–94.